ADVANCES IN ATMOSPHERIC SCIENCES, VOL. 27, NO. 2, 2010, 303–314

Comparisons of Soil Moisture Datasets over the Tibetan Plateau and Application to the Simulation of Asia Summer Monsoon Onset

BAO Qing*[1] (包 庆), LIU Yimin[1] (刘屹岷),
SHI Jiancheng[2] (施建成), and WU Guoxiong[1] (吴国雄)

[1]*State Key Laboratory of Numerical Modeling for Atmospheric Sciences and Geophysical Fluid Dynamics, Institute of Atmospheric Physics, Chinese Academy of Sciences, Beijing* 100029

[2]*Institute for Computational Earth System Science, University of California, Santa Barbara, USA*

(Received 30 August 2008, revised 8 June 2009)

ABSTRACT

The influence of soil moisture on Asian monsoon simulation/prediction was less studied, partly due to a lack of available and reliable soil moisture datasets. In this study, we firstly compare several soil moisture datasets over the Tibetan Plateau, and find that the remote sensing products from the Advanced Microwave Scanning Radiometer for Earth Observing System (AMSR-E) can capture realistic temporal variations of soil moisture better than the two reanalyses (NCEP and ECMWF) during the pre-monsoon seasons. Using the AMSR-E soil moisture product, we investigate the impacts of soil moisture over the Tibetan Plateau on Asian summer monsoon onset based on a Spectral Atmospheric Model developed at IAP/LASG (SAMIL). Comparison between results with and without the assimilation of remotely sensed soil moisture data demonstrates that with soil moisture assimilated into SAMIL, the land-sea thermal contrast during pre-monsoon seasons is more realistic. Accordingly, the simulation of summer monsoon onset dates over both the Bay of Bengal and South China Sea regions are more accurate with AMSR-E soil moisture assimilated. This study reveals that the application of the soil moisture remote sensing products in a numerical model could potentially improve prediction of the Asian summer monsoon onset.

Key words: soil moisture, remote sensing, AMSR-E and ASM onset

Citation: Bao, Q., Y. M. Liu, J. C. Shi, and G. X. Wu, 2010: Comparisons of soil moisture datasets over the Tibetan Plateau and application to the simulation of Asia summer monsoon onset. *Adv. Atmos. Sci.*, **27**(2), 303–314, doi: 10.1007/s00376-009-8132-5.

1. Introduction

Soil moisture plays an important role in land-atmosphere interactions. Numerical results derived from both a simple general circulation model (Yeh et al., 1984) and Global Land Atmosphere Coupling Experiments (Koster et al., 2004) suggest that strong land-atmosphere coupling can be modified by soil moisture, and its anomalies can persist for months.

Currently, the shortage of reliable soil moisture datasets has become a major obstacle to studying the impact of soil moisture on weather/climate variability. The Project for Inter-comparison of Land-surface Parameterization Schemes and Global Soil Wetness Project has suggested that no model is able to give a perfect simulation for the temporal and spatial variations of soil moisture (Ma et al., 2001). Since the brightness temperature can vary noticeably with the presence of soil moisture, remote sensing has been an state-of-the-art technique to obtain a large-scale temporal and spatial characterization of soil moisture fields. But current satellite remote sensing data products have uncertainties due to imperfect instrument calibration and inversion algorithms, geophysical noise, representation error, communication breakdowns, and other sources. Therefore, it is essential to

*Corresponding author: BAO Qing, baoqing@mail.iap.ac.cn

validate remotely sensed soil moisture data sources to confirm their accuracy.

Previous observational studies have exhibited the impacts of the Tibetan Plateau (TP) thermal forcing on the Asian summer monsoon (ASM) onset (Wu and Zhang, 1998; Ye and Wu, 1998; Liang et al., 2006). Generally speaking, there has been an increase of sensible heat flux and changes in the temperature-pressure fields over the TP during the ASM onset period until the monsoon reaches the TP region. Meanwhile, it is also due to the thermal and dynamic forces of the TP that the Bay of Bengal (BOB) is the region where the ASM onset generally first begins (Nitta, 1983; Luo and Yanai, 1984; Wu and Zhang, 1998; Ye and Wu, 1998; Mao et al., 2002). Since soil moisture variations lead to increases/decreases of the near surface sensible and latent heat fluxes (namely, by influencing the land surface thermal forcing), this will affect the ASM onset. In addition, the anomaly of the land surface thermal forcing can also persist for months because of the soil moisture's seasonal "memory" (Yeh et al., 1984; Koster et al., 2004). Consequently, predictions for the ASM onset may potentially be improved if the effects of the soil moisture are considered.

This study aims to deal with the following two issues: one is to compare soil moisture products over the TP; the other is to apply these datasets to investigate the impacts of the TP soil moisture on the simulation of the ASM onset. The remote sensing products used here are retrieved from the Advanced Microwave Scanning Radiometer-Earth Observing System (AMSR-E). Nevertheless, AMSR-E remote sensing products have been shown to be disturbed greatly by cell phone signals in most regions with large population. However, due to the unique surface conditions of the TP and lesser influences from cell phone signals, the TP is considered to be an idealized region to retrieve reliable remote sensing products. The atmospheric model used in this study is the Spectral Atmosphere Model of IAP/LASG (SAMIL) (Wu et al., 1996; Wang et al., 2005; Bao et al., 2006), which is an atmospheric component of the FGOALS-s climate system model (Zhou et al., 2007). In the second section, we compare the remote sensing products of soil moisture and two reanalyses with *in situ* ground observations over the TP. An introduction to the SAMIL model and the behavior of the ASM onset in SAMIL are given in the third section. The numerical experiments for ASM onset are carried out and the relevant physical mechanism is discussed in the fourth section. Finally, a discussion and summary are contained in the last two sections.

2. Datasets and comparisons

2.1 *Description of datasets*

The remote sensing products used in the study are retrieved from AMSR-E on board the AQUA satellite launched in 2002. Generally, microwave brightness at lower frequencies is more sensitive to the near surface soil moisture. The instrument differs from earlier global remote sensing products of soil moisture retrieved from the Special Sensor Microwave/Imager (SSM/I) at frequencies of 19 and 37 GHz. Instead, the AMSR-E products are retrieved from the low frequency microwave band at 6 and 10 GHz. The AMSR-E products used in this study are from National Snow and Ice Data Center. The products are generated on a fixed grid with a relatively high horizontal resolution (25-km nominal grid spacing), and a temporal resolution of twice daily, because of the ascending and descending orbital tracks (Njoku et al., 2003).

Two suites of reanalysis datasets, including the National Centers for Environmental Prediction/National Center for Atmospheric Research (NCEP/NCAR) reanalysis 1 with a daily interval (Kalnay et al., 1996) and the European Center for Medium range Weather Forecasting (ECMWF) product with a 6-hour interval (Uppala et al., 2005) are used for the cross-comparsion of AMSR-E. The spatial resolution is $2.5^\circ \times 2.5^\circ$ for NCEP and $1^\circ \times 1^\circ$ for ECMWF, respectively.

In situ ground observations of soil moisture are employed as a measure to qualitatively evaluate the AMSR-E products and the reanalyses, and are derived from CEOP (Coordinated Enhanced Observ-

Table 1. The site description of the ground measurements.

Site	Lon, Lat	Elevation (m)	Description of location	Vegetation status	Soil composition
Gêrzê	32°30′N, 84°05′E	4420	Gêrzê weather station	Sparse	Silver sand soil, mainly made up of sand and stone.
D66	35°31′N, 93°47′E	4560	It is located in foreside of ice water proluvial fan before Kunlun Mountains, Close to the 66 crossing on Tibetan Road	Medium	Soil is made up of even gravel, which of largest diameter 15–20 cm. Groundwater is 2.30 m under the ground.

ing Period) Asia-Australia monsoon project (CAMP) data (Yang et al., 2003). Since the *in situ* ground datasets are very sparse over the TP, here we select two CEOP/CAMP-Tibet sites, D66 and Gêrzê, as benchmarks for the comparisons of soil moisture products. Due to a malfunction of instrument of D66, the *in situ* ground observations there are only available after September 2003. Because of the limitations of the remote sensing inversion algorithm, AMSR-E soil moisture is not retrievable where significant fractions of snow cover, frozen ground, dense vegetation, precipitation, open water, or mountainous terrain appear within the sensor footprint (as determined by a classification algorithm and ancillary information) (Njoku et al., 2003). Table 1 shows the description of the selected site conditions. Gêrzê is located to the west of the TP in a semidesert region and D66 is to the north of the TP in a tundra meadow region. Therefore, both sites are suitable for the validation of the AMSR-E soil moisture.

2.2 *Comparisons*

To unify the comparisons, both the reanalysis datasets and the AMSR-E remote sensing products are interpolated onto the same grid as the ground measurements using bilinear interpolation. Figure 1 shows time series for the four sources of soil moisture data in D66 and Gêrzê from 1 January 2003 to 31 December 2003. Compared with the CAMP/Tibet ground observations, both ECMWF and NCEP reanalyses evidently overestimated soil moisture at both sites during the whole year. It is found that AMSR-E gives the best result during the pre-monsoon season (from 1 January to 30 April), while it underestimates soil moisture during the summer (from June to September). In addition, the AMSR-E soil moisture product can capture the small temporal variation realistically but the reanalyses cannot. Figure 2 shows the spatial pattern of the soil moisture over the TP during the

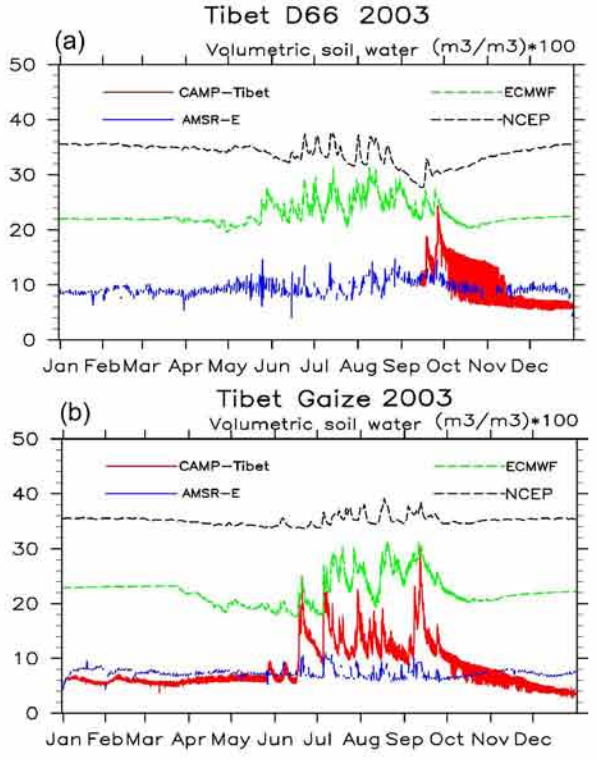

Fig. 1. Time series of soil moisture at (a) D66 and (b) Gêrzê in 2003, with four different datasets including CEOP/CAMP-Tibet *in situ* ground measurements (red solid line), AMSR-E product (blue solid line), ECMWF reanalysis (green dash line), and NCEP reanalysis (black dash line). Units of soil moisture are 10^2 m^3 m^{-3}.

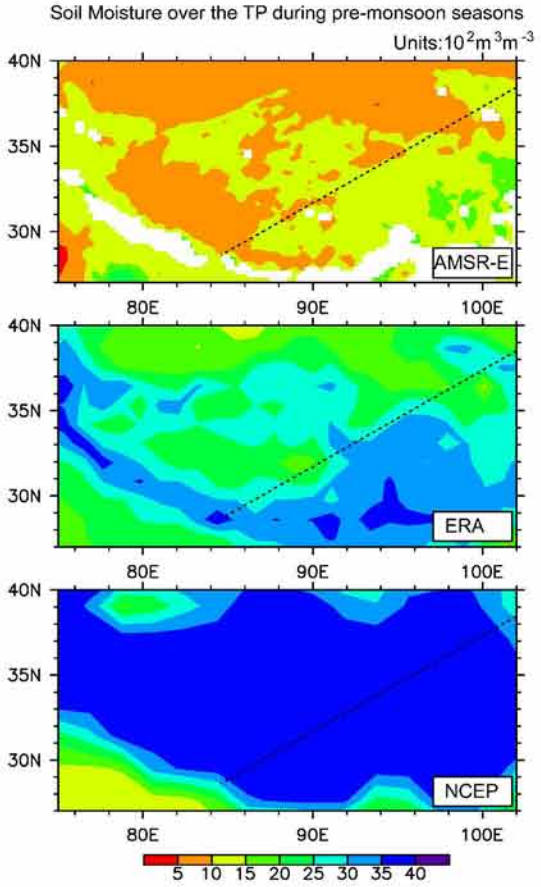

Fig. 2. The spatial pattern of the soil moisture over the TP regions in the pre-monsoon season (averaged from 1 January 2003 to 30 April 2003). The upper panel is from the AMSR-E product, the middle panel is from the ECMWF reanalysis, and the bottom panel is from the NCEP reanalysis. Units of soil moisture are 10^2 m^3 m^{-3}. The dashed lines in each pattern indicate the dry-wet contrast between the northwest and southeast parts of the TP region.

pre-monsoon season (from 1 January 2003 to 30 April 2003), and the results indicate that AMSR-E remote sensing product can reasonably identify a dry-wet contrast between the northwest and southeast parts of the TP (Kaihotsu and Koike, 2005) which is more robust than the reanalyses. The better performance of AMSR-E soil moisture during the pre-monsoon season should improve the ASM onset simulation after such data is introduced in a numerical simulation.

3. Application to the simulation of ASM onset

3.1 *Description of SAMIL AGCM*

SAMIL is a spectral transform model with 26 atmospheric layers extending from the surface to 2.19 hPa, and its spatial resolution is a rhomboidal truncation with maximum wavenumber 42 (approximately 2.81° lon×1.66° lat). SAMIL, as an atmospheric component of the climate system model FGOALS-s developed in LASG/IAP, is driven by the 5th generation of NCAR Coupler. Thereby, as one part of this coupler, NCAR CLM2 is used as a land surface component (Dai et al., 2003; Bao et al., 2006). The radiation scheme is the Slingo-Edwards parameterization (Edwards and Slingo, 1996). A modified version of the Tiedtke mass flux cumulus parameterization is utilized for deep, shallow, and midlevel convection (Tiedtke, 1989).

3.2 *Climatological ASM onset in SAMIL*

A 22-year AMIP type experiment was carried out with SAMIL. The model is integrated from 1978 to 1999, forced by real-time optimum interpolation SST (Reynolds and Marsico, 1993). The simulation of the ASM onset is evaluated by the observational results, which are derived from NCEP, the Climate Prediction Centers Merged Analysis of Precipitation (CMAP) (Xie and Arkin, 1997), and the Global Precipitation Climatology Project (GPCP) (Xie et al., 2003).

Previous studies have demonstrated that the onset of the Asian monsoon consists of three major stages, in turn including the onsets in the BOB, Southern China Sea (SCS), and Southern Asian Monsoon (SAM) regions (Wu and Zhang, 1998; Ye and Wu, 1998; Liu et al., 2002; Wang and Fan, 1999). Monsoon onset has been defined by different indices in the previous studies (e.g., Tanaka, 1992; Lau and Yang, 1997; Webster et al., 1998; Wang and Fan, 1999; Fasullo and Webster, 2003; Wang et al., 2004) and there is no agreement regarding the definitions of observed climatological monsoon onset date. Therefore, we apply both circulation and precipitation indices to evaluate model results. On the one hand, the lower level zonal flow (the 850 hPa zonal winds, hereafter "U850") is selected as one typical circulation index to depict the ASM onset, which is simple yet effective (Wang et al., 2004). Accordingly, the monsoon onset indices over BOB and SCS are respectively the mean U850 averaged within (5°–15°N, 90°–100°E) and (10°–20°N, 110°–120°E), while the index over SAM is the difference between (5°–15°N, 40°–80°E,) and (20°–30°N, 70°–90°E) (Wang and Fan, 1999). The climatological ASM onset revealed by these indices is manifested in Fig. 3. Compared to the observations, the climatological onset date of the ASM in these three key regions can be well captured in simulation, although onset is about 5 days early over the SCS.

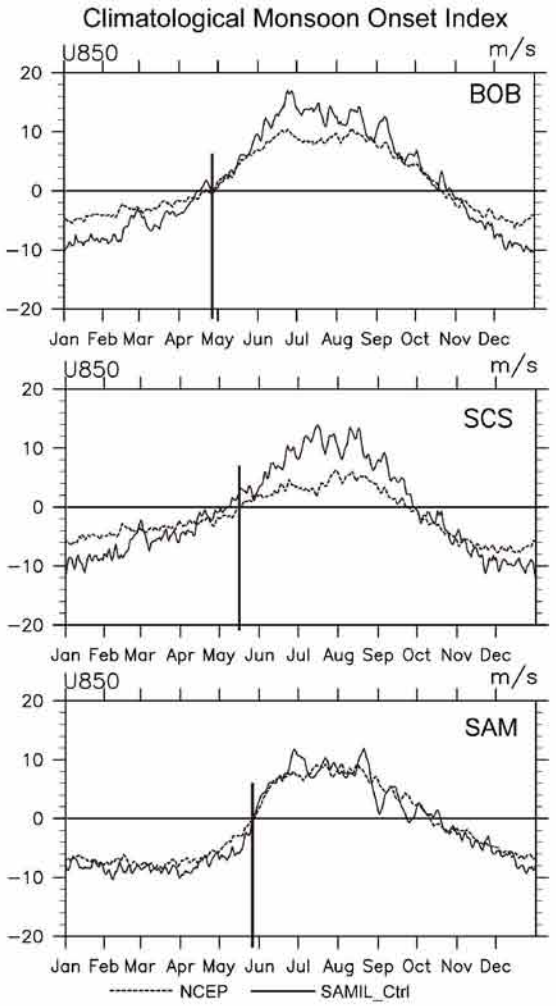

Fig. 3. The time series of index of ASM onset in Bay of Bengal (BOB), South China Sea (SCS), and South Asian Monsoon (SAM) regions. The dashed lines are the results from the NCEP reanalysis, the thin solid lines are derived from the control run of SAMIL, and the thick solid lines highlight the onset date derived from NCEP reanalysis.

On the other hand, precipitation is another typical index to describe ASM onset (Ananthakrishnan and

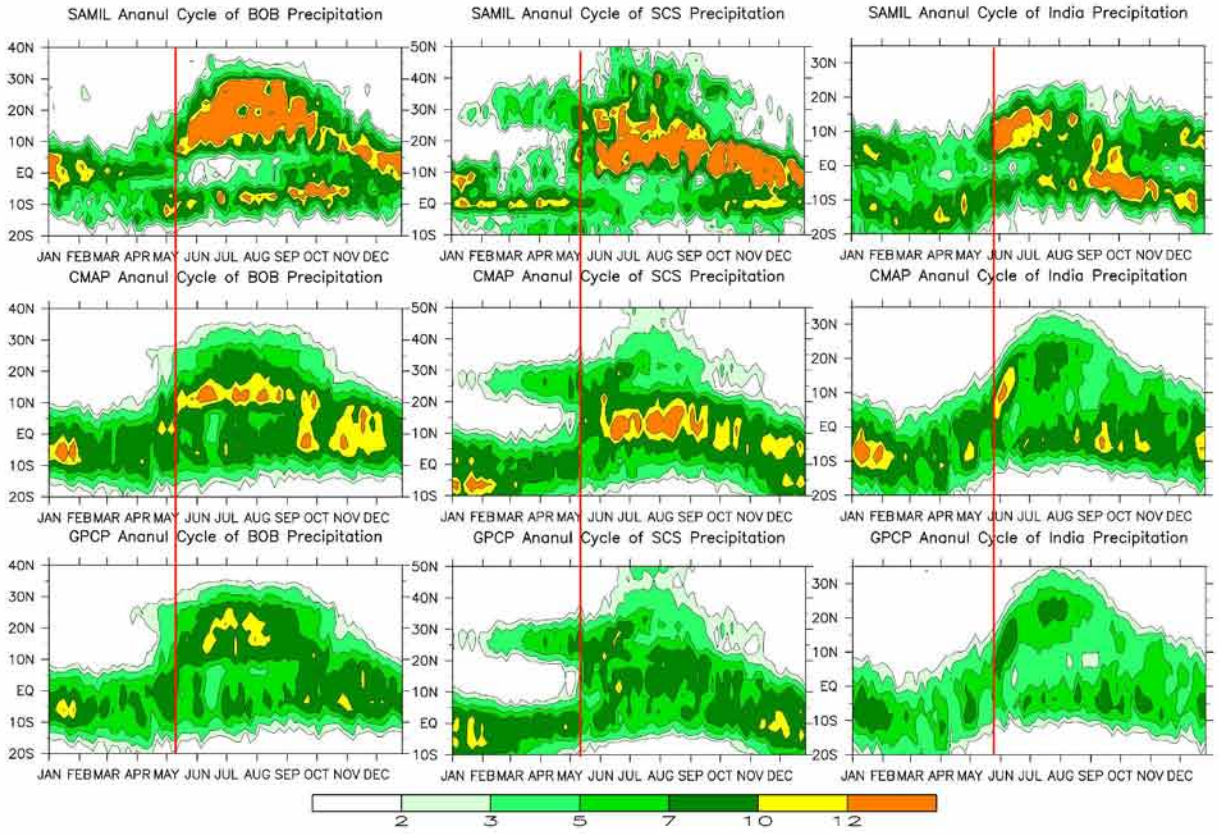

Fig. 4. The time-latitude distributions of zonal averaged precipitation over BOB (90°–100°E), SCS (110°–120°E), and SAM/India (65°–85°E) from the control run of SAMIL (upper panel), CMAP (middle panel), and GPCP (lower panel), in units of mm d^{-1}. The red line is the date of monsoon onset in the individual regions judged from CMAP and GPCP datasets.

Soman, 1988; Wang and LinHo, 2002; Zhang et al., 2002). We selected the latitude-time distributions of zonal mean precipitation in these three key regions as another measure to validate the monsoon onset, which is shown in Fig. 4. The ASM onset is characterized by an abrupt increase in precipitation. As illustrated in Fig. 4, this feature can be easily identified in the model output over the three key areas and the simulated onset date is consistent with CMAP and GPCP (red lines in Fig. 4). However, the amplitude of precipitation is overestimated compared with the observations.

3.3 *The methods of data assimilation and numerical simulation*

There will be soil moisture drift or overflow in a model if remote sensing products are introduced into the model directly. It is necessary, therefore, to apply remote sensing products using data assimilation. In this study, a nudging scheme is used to introduce the thermal conditions over the TP. It has been shown that nudging is an effective scheme to control soil moisture drift on the seasonal scale (Viterbo, 1996), and it is a flexible algorithm, which can lead to improvements in the performance of the model but with only a small increase in the amount of computation (Paniconi et al., 2003).

Two numerical experiments are carried out with SAMIL AGCM: a sensitivity run with nudging and a control run. We continue to integrate SAMIL AGCM after the 22-year AMIP type run, which has been documented in the section 3.2, but the model is forced with real-time weekly SST from 1 January 2000 to 31 December 2002 as a spin-up process. The second stage of the experiments continues following the spin-up, from 1 January 2003 onward. Both sensitivity and control experiments of the ASM onset are carried out by integrating the model from 1 January 2003 to 31 December 2003. In the "Nudging" case, a Newtonian nudging scheme is applied to assimilate AMSR-E soil moisture over the TP during the first 4 months (from January to April) of the pre-monsoon seasons. The TP region is defined as a rectangle bounded by 27°–37.5°N and 75°–102°E. Since there is around 2 hours local time difference across the TP region zonally, 2 hours is selected as the length of the assimilation window. The relaxation coefficient is set to 1/6 because 20 minutes

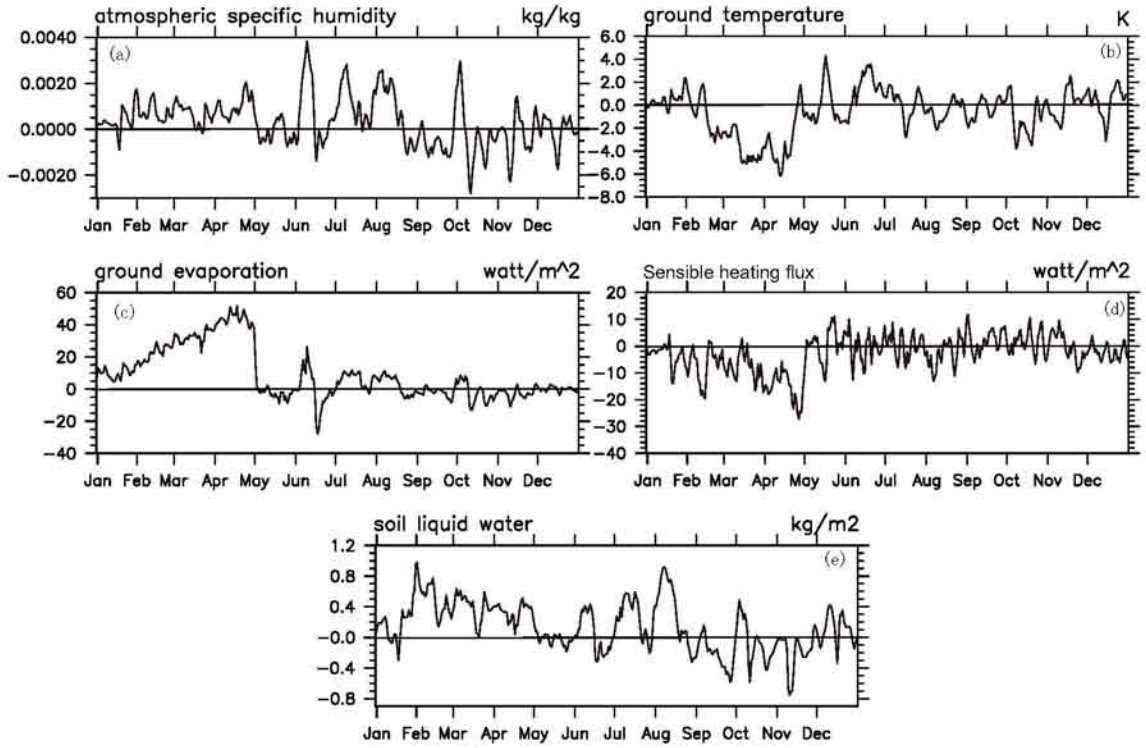

Fig. 5. The time series of difference between "Nudging" and "Ctrl" runs: (a) atmospheric specific humidity in units of kg kg^{-1}; (b) ground temperature in units of K; (c) ground evaporation in units of W m^{-2}; (d) sensible heat flux in units of W m^{-2}; (e) soil liquid water in units of kg m^{-2}.

has been selected as the length of each time step in CLM. The nudging algorithm is used twice per day according to the temporal resolution of the AMSR-E products. Both "Nudging" and "Ctrl" cases are forced with real-time weekly SST as during spin-up and are integrated via parallel mode.

3.4 *The simulation of ASM onset*

Figure 5 shows the differences, averaged over the TP, between the "Nudging" and "Ctrl" cases, which illustrates the effects of AMSR-E soil moisture over the TP. The differences of the surface energy budget are remarkable. Since the model has a dry bias in the "Ctrl" case, the "Nudging" case, which assimilates the more realistic AMSR-E moisture data, is wetter than the "Ctrl" case during the period of nudging. Increasing the soil liquid water (Fig. 5e) leads to enhanced ground evaporation (Fig. 5c) and enhances atmospheric specific humidity (Fig. 5a), but reduces the sensible heat flux (Fig. 5d) in the TP region. In addition, the wet-surface condition also leads to a cool ground temperature (Fig. 5b). These effects are consistent with previous numerical studies (Shen et al., 1998; Qian et al., 2003; Bao et al., 2006). To some extent, the consistency among atmosphere-land variables/fluxes in the model verifies the usability of the nudging procedure.

Figure 6 presents both the circulation indices and zonal averaged precipitation of the "Nudging" and "Ctrl" experiments in these three key regions, and the red dashed lines highlight the onset date derived from the observation. In the "Ctrl" run (without nudging by ASMR-E soil moisture), there is an event of abrupt westerlies associated with the rapid increase of precipitation in the 20th pentad of 2003 (which is the second pentad of April 2003, shortened here as "P20") over the BOB, which indicates the onset of the BOB monsoon, followed by a 30-day dry phase. Estimated in the same way, the onset of the monsoon is P21 (third pentad of April) over SCS and P29 (fifth pentad of May) over SAM. As in the observation, however, the onset of monsoon is P25 (first pentad of May) over BOB, P27 (third pentad of May) over SCS, and P32 (second pentad of June, which is consistent with the onset date derived from datasets of the Arabian Sea Monsoon Experiment-II (Singh et al., 2007). In that study, they concluded that SAM onset is around 7 June in 2003). In the "Ctrl" case, the early onsets of the BOB monsoon and the subsequent SCS monsoon are mainly due to the unrealistic simulation of a wet event during early April, which accompanies an abrupt event featured with strengthened westerlies in the lower troposphere.

In the "Nudging" run (with nudging toward

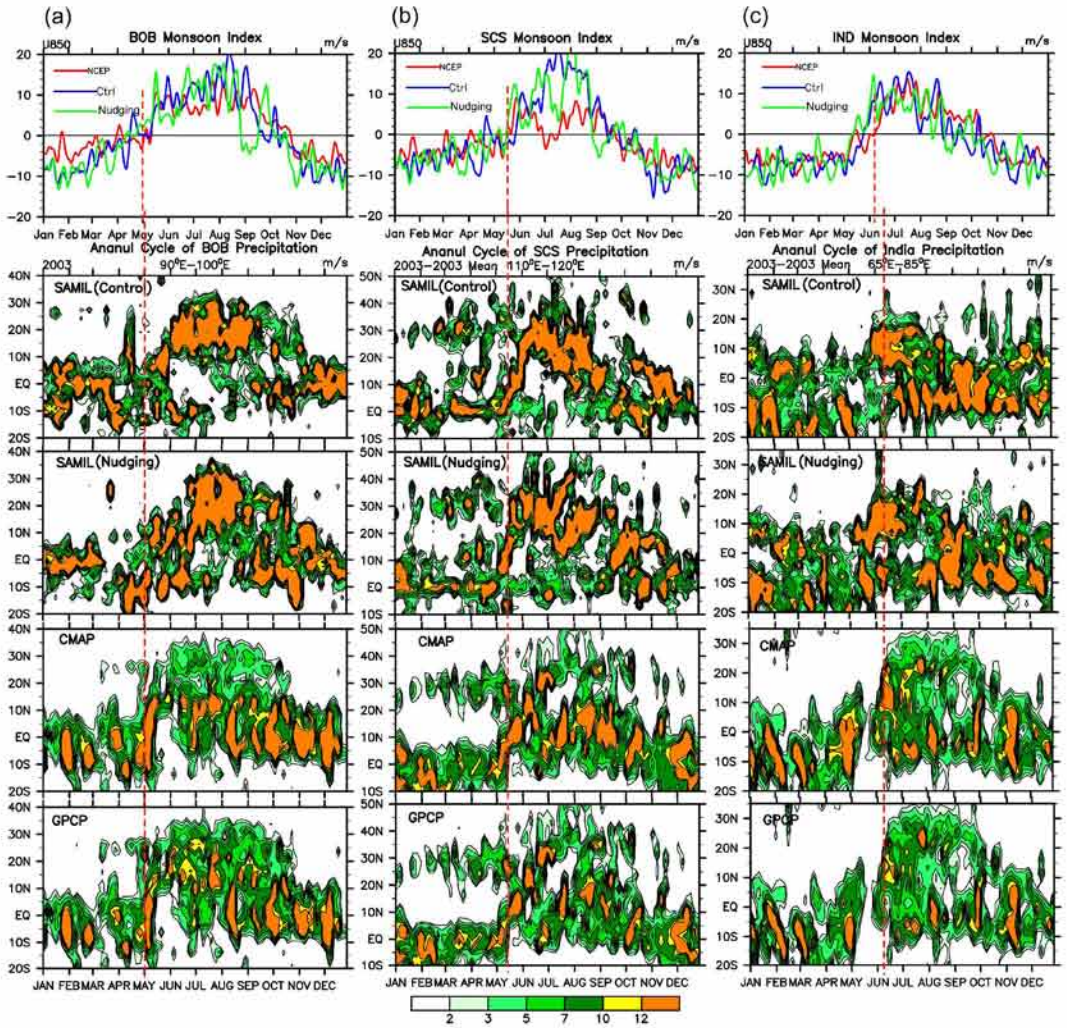

Fig. 6. The simulation of ASM onset and the corresponding observations in (a) BOB, (b) SCS, and (c) SAM/IND. The upper panels show the indices of the ASM onset derived from NCEP reanalysis (red solid lines), "Ctrl" (blue solid lines), and "Nudging" (green solid lines); the lower panels are the time latitude distributions of zonal averaged precipitation in each key region of ASM onset. The observed circulation index of the ASM onset is derived from NCEP reanalysis and the precipitation datasets are CMAP and GPCP, in units of mm d^{-1}. The dashed red lines indicate the onset date of the ASM derived from the observations.

ASMR-E soil moisture values), there is a distinct improvement in terms of the simulated ASM onset over the BOB and SCS regions. Both circulation indices and zonal mean precipitation in the "Nudging" case indicate that the simulated onset dates of the monsoon are P25 over BOB and P27 over SCS respectively, which are consistent with the observed onset pentads (highlighted with red dashed lines). This also fails, however, to simulate the onset of SAM precisely. Compared with the observations, the phasing is two pentads ahead for SAM onset, and the simulated onset date of SAM is P29. Namely, after assimilating AMSR-E remote sensing products of soil moisture, the capabilities of simulating ASM onset have been improved over the BOB and SCS regions, but are unnoticeable over the SAM region.

How does the TP soil moisture influence the ASM onset? As is well known, the modulation of the land-sea thermal contrast caused by the variation of solar zenith angle is a fundamental reason for the formation of the ASM. Considering the employment of real-time SST, the realistic thermal effect of land will give a reasonable thermal contrast. Previous studies (e.g., Pitman, 2003) show that increasing the soil moisture could enlarge the latent heat flux and reduce sensible heat flux, with the surface becoming cooler. These consequences do occur in the "Nudging" run. As shown in Figs. 5 and 7, after nudging the model

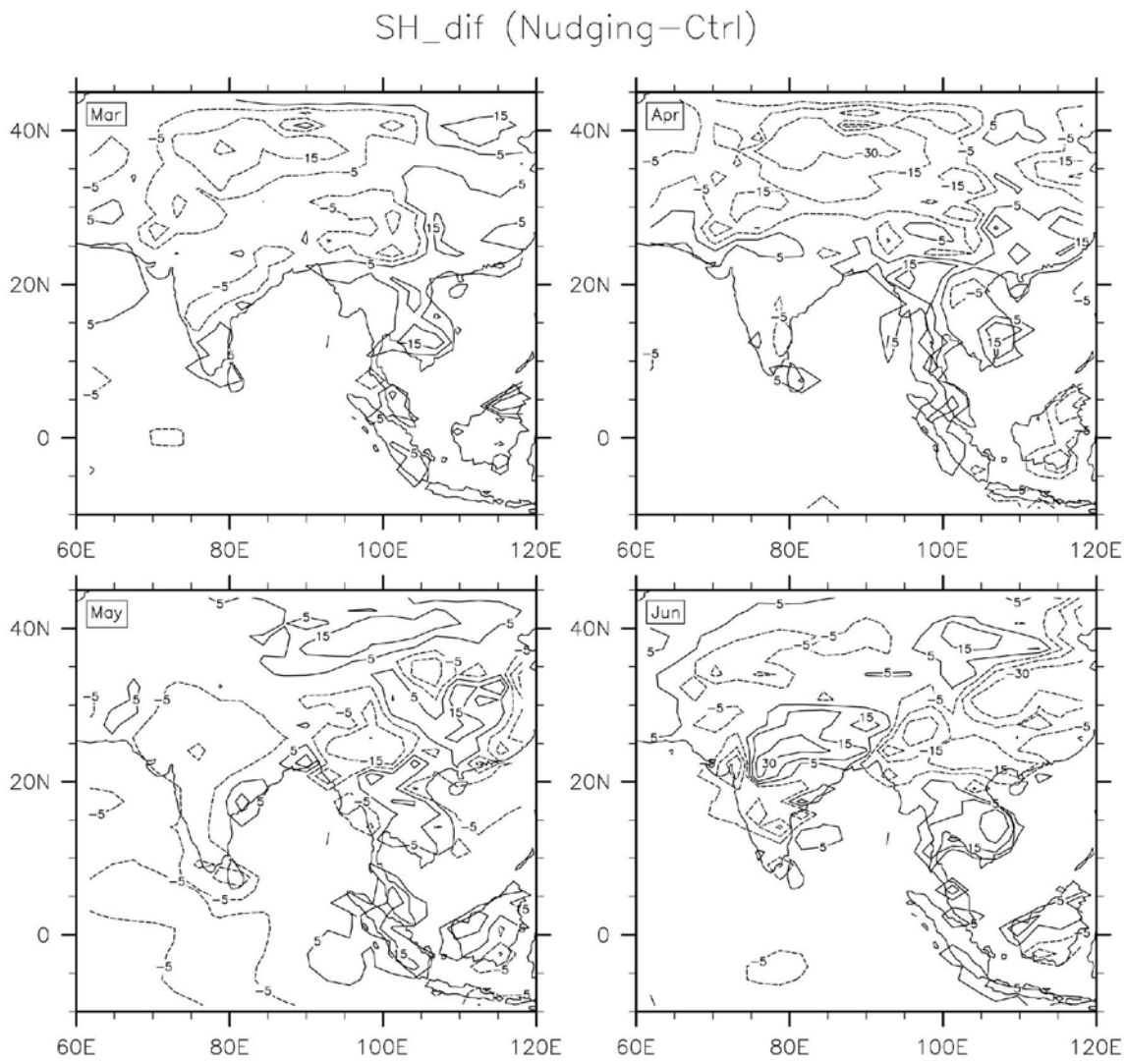

Fig. 7. The different sensible heat fluxes between "Nudging" and "Ctrl" runs from March to June in units of W m^{-2}. The dashed lines are negative and the solid lines are positive.

toward the ASMR-E soil moisture, the soil liquid water increases, and the positive anomaly can extend for the next four months. Then the sensible heat flux and surface temperature decrease ahead of the onset of monsoon. Due to the Rossby responses to the negative boundary heating anomalies over the TP, there is a large continental thermal cyclonic circulation in the lower troposphere over the East Asian region, which persists from March to April (Fig. 8). Over the BOB and SCS regions, there are easterly anomalies prevailing as the south part of the lower level continental low. Therefore, the onset of monsoon over the BOB and SCS regions becomes late, namely, the onset time becomes more realistic compared with the analysis from the observations. On the other hand, the thermal characteristics of the Tibetan Plateau and its neighboring regions are changed due to the inclusion of AMSR-E soil moisture (Figs. 5 and 7). The onset of the BOB monsoon is directly linked to the thermal as well as mechanical forcing of the Tibetan Plateau. In detail, as illustrated in Fig. 7, the sensible heat flux in the "Nudging" case is reduced in early spring (March and April) over the TP regions with an amplitude of -30 W m^{-2} in April. During the pre-monsoon season, thereby, the unrealistic strong thermal effects of the TP in the "Ctrl" run are evidently reduced in the "Nudging" run. Then, the thermal ridge in the lower troposphere subsequently turns around slowly compared with the result from "Ctrl" (not shown here, but this can be estimated from the difference of surface temperature). Therefore, as illustrated in Fig. 6a, the virtual perturbation of the circulation index disappears and zonal averaged precipitation can match the observations very well in the "Nudging" run. The

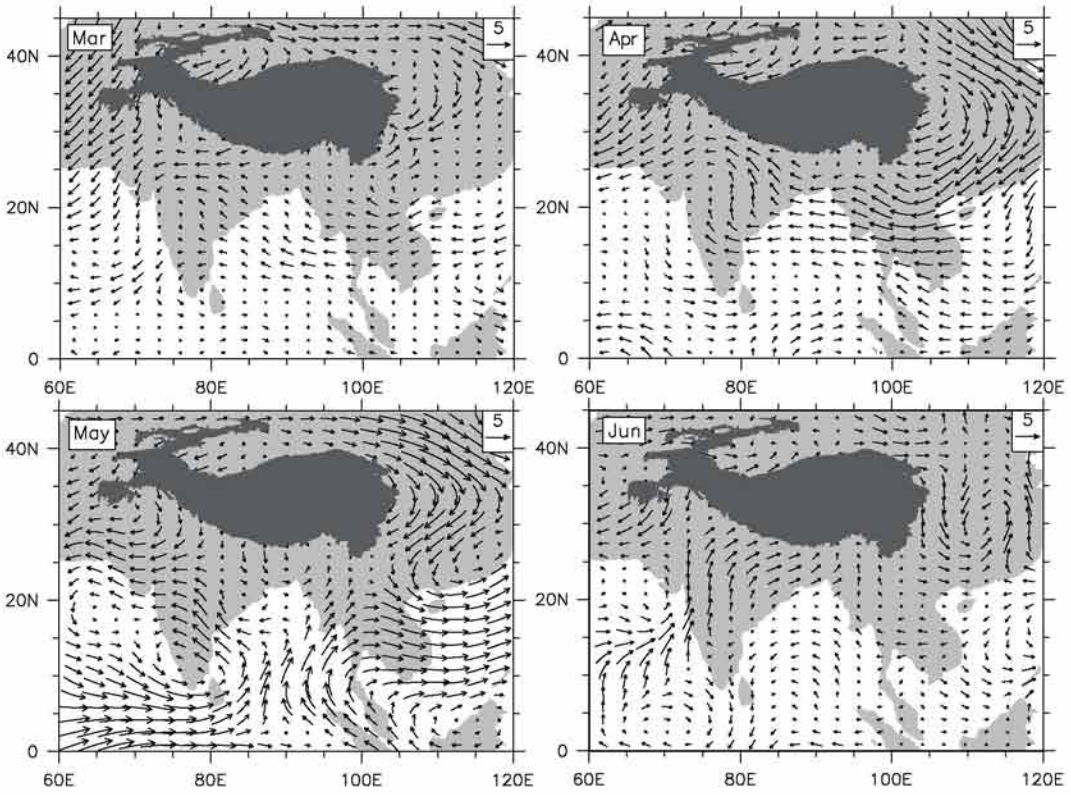

Fig. 8. Wind fields at 850 hPa between the "Nudging" and "Ctrl" runs from March to June in units of m s^{-1}. The deep shading indicates the regions of the Tibetan Plateau with elevation over 2500 km.

latent heating of the monsoon rainfall over BOB is favorable for westerlies over SCS through the asymmetrical Rossby response (Liu et al., 2002). Thus, the simulation of the ASM onset in SCS is more realistic due to the improvement of the simulation of westerly flow. However, both numerical experiments have failed to reproduce the onset event in SAM, which indicates the relationship between the thermal condition of the TP and ASM onset over the SAM regions is not the same as for BOB and SCS. These results are consistent with the evidence found in observational data reanalysis (Mao et al., 2002).

4. Discussion

In order to predict the ASM onset well by including the remote sensing products, there are still several obstacles we have to deal with. Firstly, different data assimilation methods may lead to quite different effects on the simulated results. As shown in Fig. 5c, the influence on the ground evaporation increases from January to April, but it sharply drops to around zero once nudging is stopped. The same phenomena can also be found for the ground temperature (Fig. 5b), which suggests that the data assimilation method for soil moisture should be improved so that the strength of the "initial shock" after assimilation can be reduced. Douville et al. (2000) studied the sensitivity of initial methods to soil moisture in ECMWF, and it was shown that nudging is very sensitive to model biases and sometimes produces unrealistic results but the optimum interpolation technique is more robust and reliable. Furthermore, Walker (1999) investigated three other data assimilation methods for soil moisture, including the Dirichlet boundary condition, hard-updating, and Kalman filtering (KF) assimilation schemes. They concluded that the KF method is the best. However, KF is too computationally demanding for use with model forecasting. Thereby, an economic and efficient method should be considered to assimilate remote sensing products so that numerical simulation or prediction can be improved in the future.

The uncertainty from the model physics package is another issue of more concern. Current models do not give a perfect simulation of the ASM (Kripalani et al., 2007), which is also true for SAMIL. There is a dry bias climatologically over the TP regions during boreal summer (Bao et al., 2006), and this may weaken the response of latent heating in the middle and upper troposphere to surface thermal anomalies. Therefore,

the upper-level responses are not as strong as those in the lower troposphere (figures not shown here).

The quality of remote sensing products also plays a key role in this numerical study. Nevertheless, our evaluation over the TP is still preliminary. In the future, more CAMP sites should also be used to make a deeper investigation of the quality of the AMSR-E remote sensing products. On the other hand, while the ASMR-E product of soil moisture possesses a reasonable large-scale temporal and spatial characterization, there is substantial room for improvement of the quality of the ASMR-E product, especially during the boreal summer. This would enhance the needs for short time scale prediction. Fortunately, another suite of products retrieved from AMSR-E will be available soon, which have been processed by scientists at University of Tokyo, and the performance of these products has been tested by CMAP-Tibet with *in situ* observations (Yang et al., 2007) and data from the CEOP Mongolian soil moisture network (Yang et al., 2009). The latter shows a scale-matched validation of soil moisture retrieved from AMSR-E with the data assimilation system at the University of Tokyo.

It has been demonstrated that soil moisture data leads to a notable improvement in modeling of the surface energy budget. To some extent, the improvements of simulation and prediction of ASM onset may benefit from the application of both advanced data assimilation methods and high quality remote sensing products.

5. Summary

This paper explores the influence of the TP soil moisture on the simulation of the ASM onset through AGCM experiments. The comparisons of soil moisture products over the TP indicates that AMSR-E products can reproduce well the total field of soil moisture during the pre-ASM season and can capture the temporal variation of soil moisture better than the NCEP and ECMWF reanalyses.

The numerical studies show that climatological characteristics of the ASM onset can be reproduced well in three key regions by SAMIL, and the onset dates simulated in SAMIL are consistent with the results derived from the reanalyses. Then, a nudging-based data assimilation method was used to study the effects of the AMSR-E soil moisture over the TP. The results indicate that reasonable soil moisture could improve the model's performance for the land surface fluxes, so that the land-sea thermal contrast becomes more reliable. Consequently, the incorrect prediction of a wet event accompanying the abrupt westerly shift over the BOB in early April does not occur, and instead precipitation features which advance northwards match the observations very well over the SCS region. Therefore, the simulation of the summer monsoon onset over both BOB and SCS regions is obviously improved by including AMSR-E remote sensing products of soil moisture. This study precursorily indicates that the application of the soil moisture remote sensing products in a numerical modeling setting could potentially improve prediction capabilities of the Asian summer monsoon onset.

Acknowledgements. We would like to thank Profs. LIU Jingmiao and YANG Meixue for sharing the *in-situ* ground measurements and two anonymous reviewers for their valuable suggestions. Our research was jointly supported by the 973 Program of China (2006CB403607), the Chinese Academy of Sciences (ZKCX2-YW-Q11-04), the National Natural Science Foundation of China (40805038, 40821092, 40890054), the National Science & Technology Pillar Program of China (2007BAC29B03) the Chinese Academy of Sciences (KZCX2-YW-Q11-04), and LASG Free Exploration Fund.

REFERENCES

Ananthakrishnan, R., and M. K. Soman, 1988: The onset of south-west monsoon over Kerala: 1901–1980. *J. Climate*, **8**, 283–296.

Bao, Q., Y. M. Liu, T. J. Zhou, Z. Z. Wang, G. X. Wu, and P. F. Wang, 2006: The sensitivity of the Spectral Atmospheric General Circulation Model of LASG/IAP to the land process. *Chinese J. Atmos. Sci.*, **30**, 1077–1090. (in Chinese)

Dai, Y. J., and Coauthors, 2003: The Common Land Model. *Bull. Amer. Meteor. Soc.*, **84**, 1013–1023.

Douville, H., P. Viterbo, J. F. Mahfouf, and A. C. M. Beljaars, 2000: Evaluation of the optimum interpolation and nudging techniques for soil moisture analysis using FIFE data. *Mon. Wea. Rev.*, **128**, 1733–1756.

Edwards, J. M., and A. Slingo, 1996: Studies with a flexible new radiation code. 1. Choosing a configuration for a large-scale model. *Quart. J. Roy. Meteor. Soc.*, **122**, 689–719.

Fasullo, J., and P. J. Webster, 2003: A hydrological definition of Indian monsoon onset and withdrawal. *J. Climate*, **16**, 3200–3211.

Kaihotsu, I., and T. Koike, 2005: Improving our understanding of climate change—Observing our water planet using AMSR and AMSR-E. Chapter 6, *Terrestrial Hydrology: Soil Moisture and Snow.* [Available online from http://sharaku.eorc.jaxa.jp/AMSR/doc/index.html]

Kalnay, E., and Coauthors, 1996: The NCEP/NCAR 40-year reanalysis project. *Bull. Amer. Meteor. Soc.*, **77**, 437–471.

Koster, R. D., and Coauthors, 2004: Regions of strong coupling between soil moisture and precipitation.

Science, **305**, 1138–1140.

Kripalani, R. H., J. H. Oh, and H. S. Chaudhari, 2007: Response of the East Asian summer monsoon to doubled atmospheric CO_2: Coupled climate model simulations and projections under IPCC AR4. *Theoretical and Applied Climatology*, **87**, 1–28.

Lau, K.-M., and S. Yang, 1997: Climatology and interannual variability of the southeast Asian summer monsoon. *Adv. Atmos. Sci.*, **14**, 141–162.

Liang, X. Y., Y. M. Liu, and G. X. Wu, 2006: Roles of tropical and subtropical land-sea distribution and the Qinghai-Xizang Plateau in the formation of the Asian summer monsoon. *Chinese J. Geophys.*, **49**, 983–992. (in Chinese)

Liu, Y. M., J. C. L. Chan, J. Y. Mao, and G. X. Wu, 2002: The role of Bay of Bengal convection in the onset of the 1998 South China Sea summer monsoon. *Mon. Wea. Rev.*, **130**, 2731–2744.

Luo, H., and M. Yanai, 1984: The large-scale circulation and heat sources over the Tibetan Plateau and surrounding areas during the early summer of 1979. Part II: Heat and moisture budgets. *Mon. Wea. Rev.*, **112**, 966–989.

Ma, Z. G., Z. B. Fu, L. Xie, W. H. Chen, and S. W. Tao, 2001: Some problems in the study on the relationship between soil moisture and climatic change. *Advances in Earth Science*, **16**, 563–568.

Mao, J. Y., G. X. Wu, and Y. M. Liu, 2002: Study on modal variation of subtropical high and its mechanism during seasonal transition part II: Seasonal transition index over Asian monsoon region. *Acta Meteorologica Sinica*, **60**(4), 409–420.

Nitta, T., 1983: Observational study of heat source over the eastern Tibetan Plateau during the summer monsoon. *J. Meteor. Soc. Japan*, **61**, 590–605.

Njoku, E. G., T. J. Jackson, V. Lakshmi, T. K. Chan, and S. V. Nghiem, 2003: Soil moisture retrieval from AMSR-E. *IEEE Trans. Geosci. Remote Sens.*, **41**, 215–229.

Paniconi, C., M. Marrocu, M. Putti, and M. Verbunt, 2003: Newtonian nudging for a Richards equation-based distributed hydrological model. *Advances in Water Resources*, **26**, 161–178.

Pitman, A. J., 2003: The evolution of, and revolution in, land surface schemes designed for climate models. *International Journal of Climatology*, **23**, 479–510.

Qian, Y. F., Y. Q. Zheng, Y. Zhang, and M. Q. Miao, 2003: Responses of China's summer monsoon climate to snow anomaly over the Tibetan Plateau. *International Journal of Climatology*, **23**, 593–613.

Reynolds, R. W., and D. C. Marsico, 1993: An improved real-time global sea-surface temperature analysis. *J. Climate*, **6**, 114–119.

Robock, A., and Coauthors, 2000: The global soil moisture data bank. *Bull. Amer. Meteor. Soc.*, **81**, 1281–1299.

Shen, X. H., M. Kimoto, and A. Sumi, 1998: Role of land surface processes associated with interannual variability of broad-scale Asian summer monsoon as simulated by the CCSR/NIES AGCM. *J. Meteor. Soc. Japan*, **76**, 217–236.

Singh, O. P., H. R. Hatwar and O. Prasad, 2007: Surface and upper air meteorological features during onset phase of 2003 monsoon. *Journal of Earth System Science,* **116**(4), 305–310.

Tanaka, M., 1992: Intraseasonal oscillation and the onset and retreat dates of the summer monsoon over the east, southeast and western North Pacific region using GMS high cloud amount data. *J. Meteor. Soc. Japan*, **70**, 613–629.

Tiedtke, M., 1989: A comprehensive mass flux scheme for cumulus parameterization in large-scale models. *Mon. Wea. Rev.*, **117**, 1779–1800.

Uppala, S. M., and Coauthors, 2005: The ERA-40 reanalysis. *Quart. J. Roy. Meteor. Soc.*, **131**, 2961–3012.

Viterbo, P., 1996: The representation of surface processes in general circulation models. Ph. D. dissertation, University of Lisbon, 201pp.

Walker, J. P., 1999: Estimating soil moisture profile dynamics from near-surface soil moisture measurements and standard meteorological data. Ph. D. dissertation, Department of Civil, Surveying and Environmental Engineering, University of Newcastle, 766pp.

Wang, B., and LinHo, 2002: Rainy season of the Asian-Pacific summer monsoon. *J. Climate*, **15**, 386–398.

Wang, B., and Z. Fan, 1999: Choice of south Asian summer monsoon indices. *Bull. Amer. Meteor. Soc.*, **80**, 629–638.

Wang, B., LinHo, Y. S. Zhang, and M. M. Lu, 2004: Definition of South China Sea monsoon onset and commencement of the East Asia summer monsoon. *J. Climate*, **17**, 699–710.

Wang, Z. Z., G. X. Wu, P. Liu, and T. W. Wu, 2005: The development of GOALS/LASG AGCM and its global climatological features in climate simulation, I: Influence of horizontal resolution. *Journal of Tropical Meteorology*, **21**, 225–237. (in Chinese)

Webster P. J., T. Palmer, M. Yanai, R. Tomas, V. Magana, J. Shukla, and A. Yasunari, 1998: Monsoons: Processes, predictability and the prospects for prediction. *J. Geophys. Res.*, **103**, 14451–14510.

Wu, G. X., H. Liu, Y. C. Zhao, and W. P. Li, 1996: A nine-layer atmospheric general circulation model and its performance. *Adv. Atmos. Sci.*, **13**(1), 1–18.

Wu, G. X., and Y. S. Zhang, 1998: Tibetan Plateau forcing and the timing of the monsoon onset over South Asia and the South China Sea. *Mon. Wea. Rev.*, **126**, 913–927.

Xie, P. P., and Coauthors, 2003: GPCP Pentad precipitation analyses: An experimental dataset based on gauge observations and satellite estimates. *J. Climate*, **16**, 2197–2214.

Xie, P. P., and P. A. Arkin, 1997: Global precipitation: A 17-year monthly analysis based on gauge observations, satellite estimates, and numerical model outputs. *Bull. Amer. Meteor. Soc.*, **78**, 2539–2558.

Yang, K., and Coauthors, 2007: Auto-calibration system

developed to assimilate AMSR-E data into a land surface model for estimating soil moisture and the surface energy budget. *J. Meteor. Soc. Japan*, **85A**, 229–242.

Yang, K., T. Koike, I. Kaihotsu, and J. Qin, 2009: Validation of a dual-pass microwave land data assimilation system for estimating surface soil moisture in semi-arid regions. *Journal of Hydrometeorology*, **10**, 780–793.

Yang, M. X., T. D. Yao, X. H. Gou, T. Koike, and Y. Q. He, 2003: The soil moisture distribution, thawing-freezing processes and their effects on the seasonal transition on the Qinghai-Xizang (Tibetan) plateau. *Journal of Asian Earth Sciences*, **21**, 457–465.

Ye, D. Z., and G. X. Wu, 1998: The role of the heat source of the Tibetan Plateau in the general circulation. *Meteor. Atmos. Phys.*, **67**, 181–198.

Yeh, T. C., R. T. Wetherald, and S. Manabe, 1984: The effect of soil moisture on the short-term climate and hydrology change: A numerical experiment. *Mon. Wea. Rev.*, **112**, 474–490.

Zhang, Y. S., T. Li, B. Wang, and G. X. Wu, 2002: Onset of the summer monsoon over the Indochina Peninsula: Climatology and interannual variations. *J. Climate*, **15**, 3206–3221.

Zhou, T. J., Y. Q. Yu, H. L. Liu, W. Li, X. B. You, and G. Q. Zhou, 2007: Progress in the development and application of climate ocean models and ocean-atmosphere coupled models in China. *Adv. Atmos. Sci.*, **24**, 1109–1120, doi: 10.1007/s00376-007-1109-3.